

On Grain Boundary Sliding and Diffusional Creep

R. RAJ AND M. F. ASHBY

The problem of sliding at a nonplanar grain boundary is considered in detail. The stress field, and sliding displacement and velocity can be calculated at a boundary with a shape which is periodic in the sliding direction (a wavy or stepped grain boundary): a) when deformation within the crystals which meet at the boundary is purely elastic, b) when diffusional flow of matter from point to point on the boundary is permitted. The results give solutions to the following problems. 1) How much sliding occurs in a polycrystal when neither diffusive flow nor dislocation motion is possible? 2) What is the sliding rate at a wavy or stepped grain boundary when diffusional flow of matter occurs? 3) What is the rate of diffusional creep in a polycrystal in which grain boundaries slide? 4) How is this creep rate affected by grain shape, and grain boundary migration? 5) How does an array of discrete particles influence the sliding rate at a grain boundary and the diffusional creep rate of a polycrystal? The results are compared with published solutions to some of these problems.

1. INTRODUCTION

Our experiments¹ have convinced us that the rate at which sliding occurs at a stressed grain boundary is frequently determined by the boundary *shape*. Briefly, the cogent observations* of the sliding at grain bound-

*Some of which have been reported also by other investigations; see the reviews of R. N. Stephens (Met. Revs. 1966, vol. 11, p. 129) and R. L. Bell and T. G. Langdon: *Interfaces*, Butterworths, 1969.

aries in copper and silver are:

- a) that a number of specimens cut from the same bicrystal show quite different steady-state sliding rates,
- b) that the sliding rate changes when the boundary alters its shape by migrating,
- c) that the precipitation of hard particles into a boundary slows down the steady-state sliding rate, and
- d) that the activation energy for grain boundary sliding is sometimes (but not always) equal to that for *bulk* diffusion.

Although more exotic explanations are possible, we have been able to explain, quantitatively, almost all our observations by supposing that the sliding rate is controlled by the accommodating processes where it deviates from a perfect plane, not by any intrinsic property of the boundary itself.

To grasp the physical meaning of the calculations contained in this paper, it may be helpful to visualize two crystals which meet at smooth, but nonplanar surfaces which mate exactly with each other. Between the mating surfaces is an extremely thin layer of viscous—though not necessarily Newtonian viscous—oil, modeling the intrinsic mechanical properties of the grain boundary. This layer transmits all normal stresses, but allows shear stress to relax with some characteristic relaxation time. The layer rarely controls the rate of sliding, though it is possible to devise experiments when it should (Section 2). Sliding generates incompatibilities where the boundary deviates from a perfect plane; almost always it is the accommodation of these

incompatibilities which controls the extent and rate of sliding.

The accommodation may be purely elastic: as sliding proceeds, elastic stresses build up at asperities on the boundary, or at places where the boundary has curvature, steps, or meets other boundaries at triple lines. The stresses ultimately grow until the appropriate component of them balances the applied stress, when sliding stops. At high temperatures, a second accommodating process is possible. The stresses developed at a nonplanar boundary by sliding can set up a diffusive flux of matter from compressed parts of the boundary to those in tension. A steady-state, diffusion-controlled, sliding then occurs. There is a third alternative. If the stresses in crystals which the boundary separates become sufficiently large, plastic flow involving dislocation motion can accommodate the incompatibility due to sliding.

This paper describes solutions for the stress field, diffusive fluxes, and rates of sliding or (where appropriate) strain-rates resulting from sliding at nonplanar grain boundaries. The two-dimensional problem is solved for a boundary of arbitrary shape, described by a Fourier series, subjected to a shear stress. Later, a number of specific and simple applications are described; these can be understood without understanding the solution of the general problem. We attempt to answer questions such as: How fast does a serrated boundary slide? How much sliding occurs when the accommodation is elastic? What is the strain-rate in a polycrystal which deforms by sliding with diffusional accommodation? How does grain shape affect this rate? How do grain boundary precipitates change the rate of grain-boundary sliding? How does grain-boundary migration influence sliding? Our results are compared with solutions to some of these problems presented by other authors.

The paper explores, in detail, aspects of grain-boundary sliding which can be treated by *continuum* theories of elasticity and diffusive flow. Microscopic or atomistic aspects of the sliding process which cannot be incorporated into continuum theories, and which are still imperfectly understood, can sometimes be important. A discussion of some of the relevant microscopic processes is given by Gleiter *et al.*² and Ashby.³

R. RAJ, formerly Graduate Student at Harvard University, Cambridge, Mass., is now Research Scientist, Chase Brass and Copper Co., Cleveland, Ohio. M. F. ASHBY is Professor, Division of Engineering and Applied Physics, Harvard University.

Manuscript submitted October 8, 1970.

2.1) SLIDING WITH ELASTIC ACCOMMODATION

The Two-Dimensional Calculation

Imagine a shear stress, τ_a , to be applied to a nonplanar boundary like one of those shown in Fig. 2.1. The shape of these boundaries, or of any boundary which has a two-fold axis of symmetry and bounded first derivatives, can be described by a cosine Fourier series

$$x = \sum_1^{\infty} h_n \cos \frac{2\pi}{\lambda} ny \quad [1]$$

If the elastic constants of the two crystals which meet at the boundary were *infinite*, the shear stress would cause no sliding. Finite elastic constants, on

the other hand, permit some sliding since relative normal displacements of the two crystals at the boundary can be accommodated by local elastic deformation of the crystals themselves. This leads (via Hooke's law) to stresses which tend to oppose further sliding, and which, growing as sliding continues, ultimately balance the applied stress and stop the sliding. When this equilibrium state is reached, only normal stresses σ_n , Fig. 2.1, act across the boundary plane: the ability of the boundary to slide has relaxed the shear component of stress.

Appendix I contains a calculation which describes the extent of this kind of sliding, and the internal stress-field generated by it. The total relative displacement, \bar{U} , in the y direction, of the two crystals before the internal stress balances the applied stress, and sliding stops, is

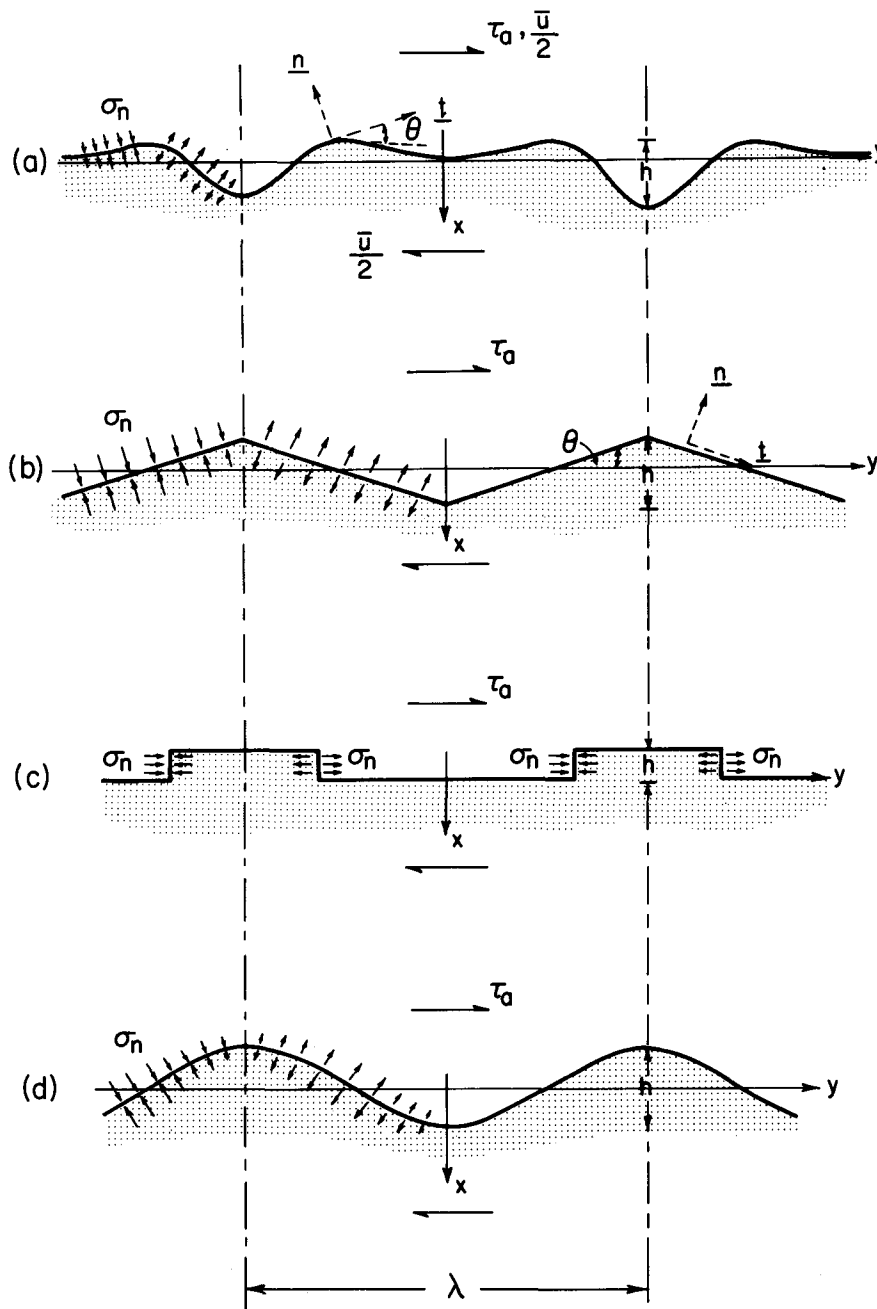


Fig. 2.1—Four examples of nonplanar boundaries. A shear-stress τ_a , causing a relative sliding displacement \bar{U} , generates a distribution of normal stress σ_n acting across the boundary surface.

$$\bar{U} = \frac{(1-\nu^2)}{\pi^3} \frac{\lambda^3}{\sum_1^{\infty} n^3 h_n^2} \frac{\tau_a}{E} \quad [2]$$

This sliding is *recoverable*; when the stress is removed the boundary will slide back. The normal stress acting on the boundary plane is given by

$$\sigma_n = - \frac{\tau_a \lambda}{\pi} \frac{\sum_1^{\infty} n^2 h_n \sin \frac{2\pi}{\lambda} ny}{\sum_1^{\infty} n^3 h_n^2} \quad [3]$$

Here ν is Poissons ratio, E Young's modulus, λ the basic wavelength of the boundary shape, Fig. 2.1, τ_a the applied stress, and h_n the Fourier coefficients of the boundary shape. If desired, the entire stress field in both crystals (not just in the boundary plane) can be obtained by the method of Appendix I.

(Before equilibrium is reached, sliding proceeds with a *velocity* which reflects the intrinsic properties of the boundary itself: the viscosity of the "oil film" referred to earlier. Damping experiments which measure the relaxation time, or some related property, when the accommodation is *purely elastic* seem to be the only way to measure the intrinsic mechanical properties of the boundary).

2.2) EXAMPLES AND DISCUSSION BASED ON THE RESULTS OF SECTION 2.1

The results given as Eqs. [2] and [3], though complicated, have considerable generality. They give the elastic sliding displacement, and the stress distribution, at any boundary with a symmetrical shape. They are accurate if the amplitude $h/2$ of the boundary waviness is small compared to its wavelength λ and remain a reasonable approximation even when h is as large as $\lambda/2$.

a) The Sinusoidal Boundary

A sine wave is often a good approximation for the shape of a wavy boundary. It is described by the first term of a Fourier series; thus the boundary of Fig. 2.1(d) is described by

$$x = \frac{h}{2} \cos \frac{2\pi}{\lambda} y$$

so that $h_1 = h/2$ and all other h_n are zero. An applied shear stress τ_a will then cause a total sliding displacement given by Eq. [2] as

$$\bar{U} = \frac{4(1-\nu^2)}{\pi^3} \frac{\lambda^3}{h^2} \frac{\tau_a}{E} \quad [4]$$

where E is Young's modulus for the crystal. This amount of sliding generates a local stress σ_n acting across, and normal to, the boundary plane. This normal stress is given by Eq. [3]; it varies sinusoidally with position in the following way:

$$\sigma_n = - \frac{2}{\pi} \frac{\tau_a \lambda}{h} \sin \frac{2\pi}{\lambda} y \quad [5]$$

b) The Internal Stresses Generated by Sliding

Sliding with elastic accommodation generates a distribution of normal stress acting across the boundary surface and given by Eq. [3]. The stress has sharp peaks where the slope of the boundary changes abruptly. Two examples are shown in Fig. 2.2: that of a saw-tooth boundary and stepped boundary. Below the boundary shapes is shown the normal stress σ_n acting on the boundary plane. When accommodation is elastic, the stress σ_n rises sharply at the corners of the saw-tooth shape, and at the steps, where they reach values of many times greater than the applied stress τ_a .

The lowest curves of the figure show how the stress is redistributed when diffusional accommodation (dis-

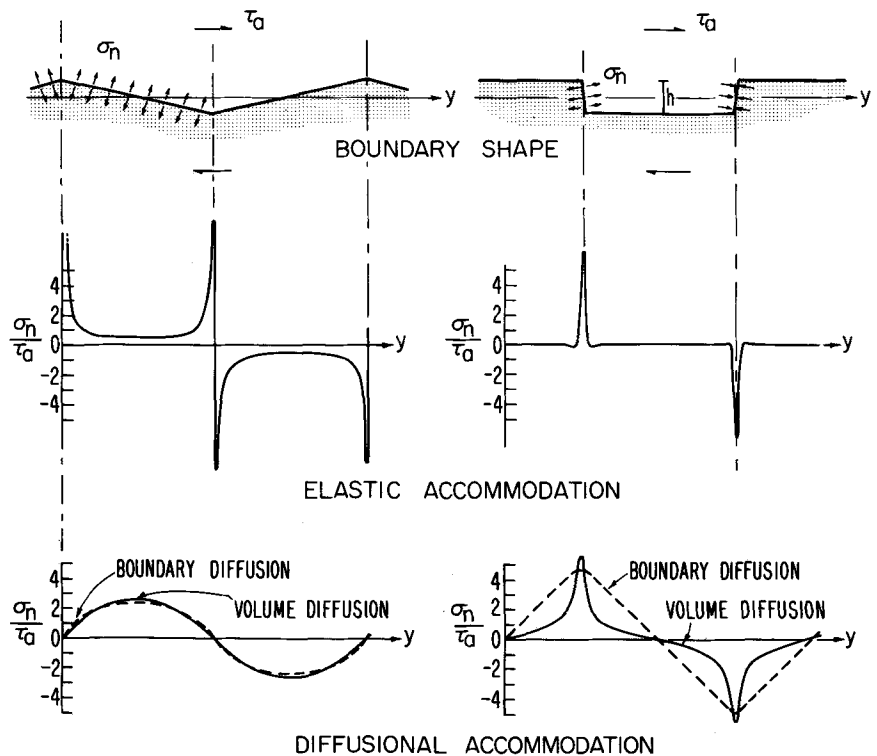


Fig. 2.2—Sliding at the saw-toothed, and at the stepped boundary shown above generates a distribution of normal stress σ_n acting across the boundary plane. The distribution when accommodation is *elastic* differs totally from that when accommodation is by *diffusion*.

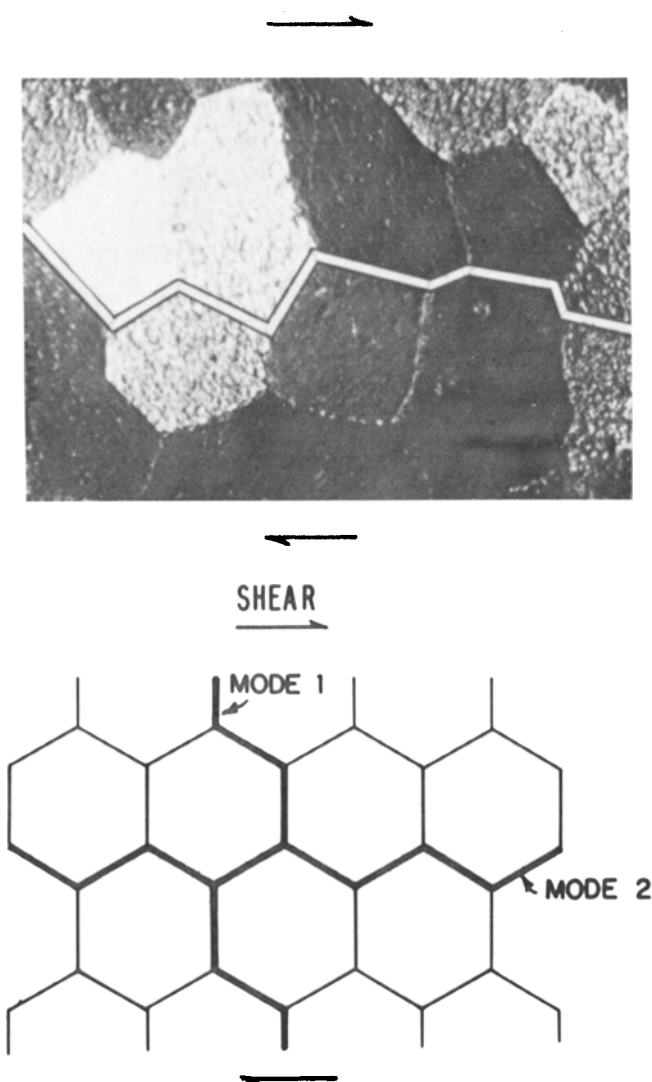


Fig. 2.3—A shear stress applied to a polycrystal causes sliding along nonplanar surfaces like that shown above. If the array of grains is idealized by a hexagonal array, two orthogonal sets of sliding surfaces (Modes 1 and 2) exist as shown below.

cussed in Section 3) is allowed: the redistribution totally changes the stress distribution. It is not generally realized that standard elastic solutions, such as those for an elastic crack, are not applicable to problems of grain boundary sliding at high temperatures (when diffusion is possible) because of this redistribution of stress.

c) Deformation of a Polycrystal: Comparison with the Results of Zener⁴ and Kê⁵

Consider the sliding which occurs when a shear stress τ_a is applied to a polycrystal of grain size d , like that shown in Fig. 2.3. As a first approximation, (though it is a poor one) the path shown on the figure can be approximated by a sine wave of wavelength $\frac{3}{2}d$ and height (h) of $d/2$. Then Eq. [4] shows that the net sliding displacement \bar{U} , in a direction parallel to the stress, is given by

$$\bar{U} = 0.87(1 - \nu^2)d \frac{\tau_a}{E} \quad [6]$$

More exactly, the two orthogonal paths labeled "Mode 1" and "Mode 2" on the figure can be described by Fourier series, and the sliding displacement evaluated for each one properly by applying Eq. [2]. The result has precisely the same form as Eq. [6], with the constant 0.87 replaced by 0.34 for Mode 1 and 0.8 for Mode 2. Taking typical values for the grain size $d \approx 10^{-2}$ cm and $\tau_a/E = 10^{-4}$, we obtain for the total sliding displacement

$$\bar{U} \approx 50\text{\AA}$$

The point here is that a boundary in a polycrystal can slide only *an extremely small distance* before internal stresses develop which oppose further sliding. The intrinsic viscosity of the boundary itself (the property of the "oil film") will only influence the rate of sliding when the sliding displacements are less than this. This viscosity may be detected in damping experiments like those of Kê⁵ when the sliding displacements are of order 10^{-6} cm, but will very rarely be measurable by normal macroscopic experiments. Instead, the rate at which *macroscopic* sliding occurs will be limited by the rate at which one of two accommodation processes—diffusion or dislocation motion—can occur.

Both the sliding modes shown in Fig. 2.3 contribute to the anelastic strain in the specimen. Since they are orthogonal, the net strain is the sum of the sliding displacements of the two modes, divided by the grain size, d :

$$\gamma^{\text{ANEL}} = 1.14(1 - \nu^2) \frac{\tau_a}{E} = 0.57(1 - \nu) \frac{\tau_a}{\mu} \quad [7]$$

where μ is the unrelaxed shear modulus. It is independent of grain size. This anelastic strain results in an apparently lower shear modulus μ_R , given by

$$\frac{\mu_R}{\mu} = \frac{1}{[0.57(1 - \nu) + 1]} \quad [8]$$

If Poisson's ratio is taken as $\frac{1}{3}$, the ratio of μ_R/μ is 0.72.

The only comparable calculation is that of Zener and Kê.^{4,5} They considered sliding with elastic accommodation for spherical grains (which, unlike our hexagonal prisms, don't pack to fill space). Their result

$$\frac{\mu_R}{\mu} = \frac{2(7 + 5\nu)}{5(7 - 4\nu)} \quad (\text{Zener, Kê})$$

reduces to 0.62 when Poisson's ratio is set equal to $\frac{1}{3}$. It is not clear at present whether the difference between the two results reflects the difference in grain shape, or is caused by the approximation inherent in our treatment.

3.1) SLIDING WITH DIFFUSIONAL ACCOMMODATION

The Two-Dimensional Problem

Steady-state sliding is possible if a diffusive flux of atoms, or vacancies, accommodates the relative displacements of the two crystals.

A simple example is shown in Fig. 3.1. A sliding rate \bar{U} in the y direction translates the upper half crystal from the position shown by the full line to that shown by the broken line, in time Δt . A sliding displacement $\bar{U}\Delta t$ can be resolved, locally, into compo-

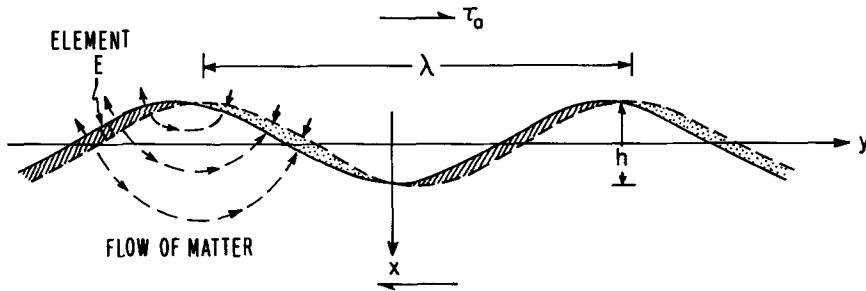


Fig. 3.1—Steady-state sliding with diffusional accommodation.

nents parallel and normal to the boundary. Steady-state sliding then requires that the net flux of atoms into or out of each element of the boundary precisely account for the normal component of the sliding displacement there. This flux of atoms (or counterflux of vacancies) is supplied by volume diffusion through the two crystals and by diffusion in the plane of the grain boundary itself. The normal stress σ_n acting on the boundary plane is now determined by the requirement of continuity: it is that stress distribution which will drive diffusive flow at a rate that exactly compensates for the normal component of displacement at each point on the boundary. In general, this distribution of normal stress is quite different from that obtained in Section 2, when no diffusion was permitted.

Appendix 2 contains a calculation which describes this kind of sliding, allowing transport by both volume and by grain-boundary diffusion. For the general boundary described by Eq. [1], the important results are as follows. The steady-state, diffusion-controlled sliding rate, \dot{U} , is given by

$$\dot{U} = \frac{2}{\pi} \frac{\tau_a \Omega}{kT} \frac{\lambda}{h^2} D_v \sum_1^{\infty} \left\{ \frac{1}{\frac{1}{n} + \frac{\pi \delta}{\lambda} \frac{D_B}{D_v}} \right\} \quad [9]$$

where h is the total height of the boundary shape, as shown in Figs. 2.1 and 3.1. The normal stress in the boundary plane, $\sigma_n(0, y)$ is given by

$$\sigma_n(0, y) = -\frac{\tau_a \lambda}{\pi h} \frac{\sum_1^{\infty} \left\{ \frac{h_n/h}{\left(1 + \frac{n\pi\delta}{\lambda} \frac{D_B}{D_v}\right)} \sin \frac{2\pi}{\lambda} ny \right\}}{\sum_1^{\infty} \left\{ \frac{nh_n^2/h^2}{\left(1 + \frac{n\pi\delta}{\lambda} \frac{D_B}{D_v}\right)} \right\}} \quad [10]$$

Here τ_a is the applied shear stress, Ω the atomic volume, D_v the bulk self-diffusion coefficient, D_B that for boundary diffusion, δ the thickness of the grain-boundary diffusion path, λ the basic periodicity of the boundary, and h_n the Fourier coefficients describing the boundary shape. The entire stress field within each crystal if desired, can be obtained by the method of Appendix 2.

3.2) EXAMPLES AND DISCUSSION BASED ON THE RESULTS OF SECTION 3.1

The two results given as Eqs. [9] and [10], though complicated, have great generality. They allow the diffusion-accommodated sliding rate, and strain distribution, at a boundary of any arbitrary shape to be calculated. They become increasingly exact as the

ratio of the amplitude $h/2$ of the boundary to its wavelength λ decreases. If h is about $\lambda/2$, the error is of the order $\sqrt{2}$. This level of accuracy is almost always adequate since diffusion coefficients, particularly those for boundary diffusion, are less accurately known than this.

a) The Sinusoidal Boundary of Wavelength λ and Amplitude $h/2$

The sinusoidal boundary is a useful approximation for any boundary with an obvious periodicity and amplitude. Its shape, illustrated by Fig. 2.1(d), is described by

$$x = \frac{h}{2} \cos \frac{2\pi}{\lambda} y$$

The sliding expression, Eq. [9], then reduces to

$$\dot{U} = \frac{8}{\pi} \frac{\tau_a \Omega}{kT} \frac{\lambda}{h^2} D_v \left\{ 1 + \frac{\pi \delta}{\lambda} \frac{D_B}{D_v} \right\} \quad [11]$$

Let the dimensionless quantity $(\pi\delta/\lambda)/(D_B/D_v) = M$. Then if M is large compared to unity, transport is mainly by boundary diffusion, and the sliding rate becomes independent of λ , and dependent on amplitude as $1/h^2$. When M is small compared to unity, volume diffusion is dominant, and the sliding rate varies as λ/h^2 . In general a short wavelength and a low temperature favor transport by boundary diffusion; a long wavelength and high temperature favor volume diffusion. Fig. 3.2 shows the sliding rate, in units of $(8/\pi)(\tau_a \Omega/kT)(D_v/\lambda)$, plotted against the "waviness" of boundary, h/λ , for various values of M . It demonstrates that, for a given M , the sliding rate decreases rapidly as the boundary becomes increasingly non-planar.

The distribution of normal stress, σ_n , acting on the boundary during steady-state sliding, from Eq. [10], is

$$\sigma_n = -2 \frac{\tau_a \lambda}{\pi h} \sin \frac{2\pi}{\lambda} y \quad [12]$$

This is precisely the same stress distribution that would have formed if no diffusion had been permitted, Eq. [5]. The sinusoidal boundary is unique in this respect; in all other cases, of which examples are given below, the stress distribution changes when diffusion occurs.

For a quick estimate of the sliding rate and stresses, at a boundary of simple shape with an obvious basic wavelength and amplitude (like those of Fig. 2.1) these expressions are adequate. They may differ by a factor of two from more exact solutions. Their usefulness and wide applicability stems from the fact that diffusional redistribution of matter quickly removes the

higher terms in the Fourier series describing the stresses at the boundary, leaving only that with the basic wavelength, λ , associated with the boundary shape. (This sort of simplification should not be applied when accommodation is elastic, since no mechanism then exists for smoothing out the stress distribu-

tion.) When, however, the basic wavelength is less obvious (e.g. a boundary containing particles with size w and spacing λ), expressions [11] and [12] should not be used. Instead a complete solution using Eq. [9], or one using results given in Section 3.2d, or Section 4 should be used.

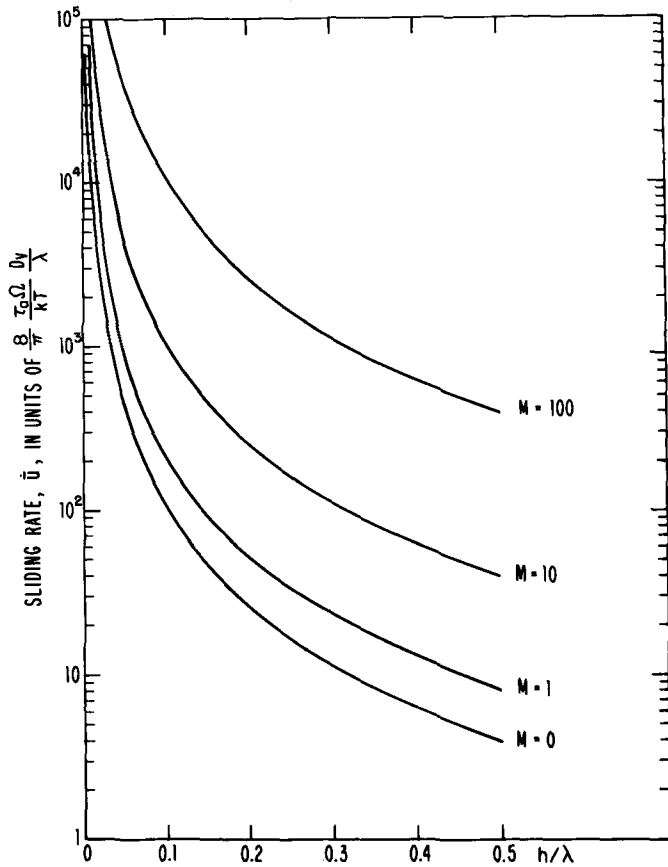


Fig. 3.2—The steady-state sliding rate at a boundary of sinusoidal shape, as a function of amplitude.

b) The Internal Stress Associated with Diffusional Accommodation

The normal stress σ_n acting across the boundary plane is given by Eq. [10]. As an example, this stress has been evaluated for two boundary shapes: the saw tooth and the stepped boundary. The results are shown at the bottom of Fig. 2.2. The normal stress differs from that formed when accommodation is purely elastic, because diffusion smooths out, and redistributes, the normal stress as described above.

c) The Periodic Stepped-Boundary: Comparison with the Results of Gifkins and Snowdon⁶

Consider the rate of sliding of the regular-stepped boundary shown in Fig. 3.3(a): by "regular" we mean that the steps are equally spaced.

If transport is by grain-boundary diffusion *only*, the basic rate equation, Eq. [9], reduces to

$$\dot{U} = 2 \frac{\tau_a \Omega}{kT} \frac{\delta}{h^2} \frac{D_B}{\sum_1^{\infty} \left(\frac{h_n}{h}\right)^2} \quad [13]$$

The square-wave boundary, shown in Fig. 3.3(a) is described by the Fourier series

$$x = \sum_1^{\infty} h_n \cos \frac{2\pi}{\lambda} ny$$

with

$$\frac{h_n}{h} = \frac{2}{n\pi} \sin \frac{n\pi}{2}$$

Substituting in Eq. [13] we obtain

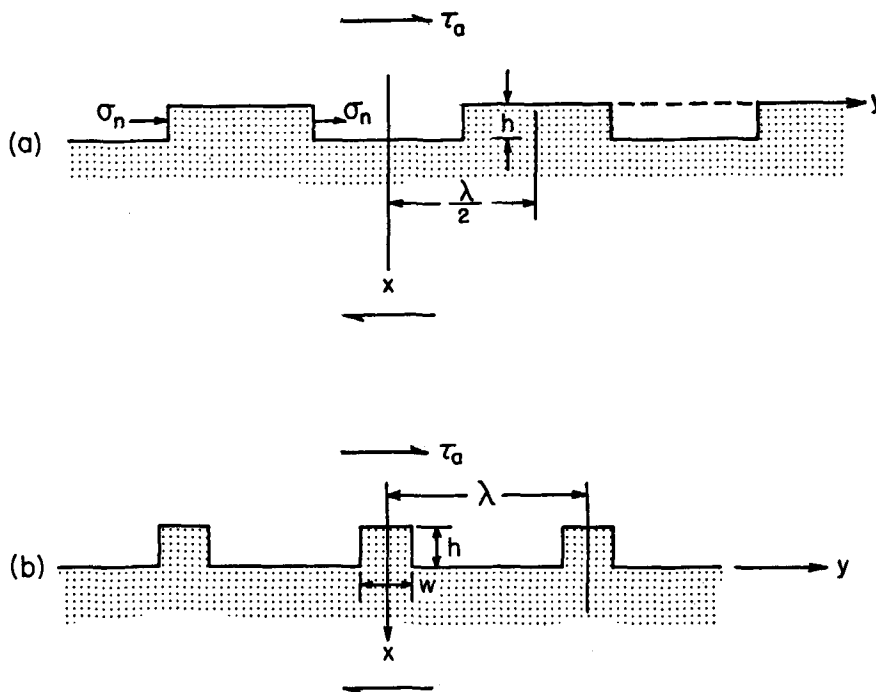


Fig. 3.3—Above: a regularly stepped boundary; below: a more general stepped boundary.

$$\dot{U} = 4 \frac{\tau_a \Omega}{kT} \frac{\delta}{h^2} D_B \quad [14]$$

Note that the square-wave shape slides at exactly half the rate of a sinusoidal shape with the same base-wavelength and amplitude, Eq. [11], and that, as before, the sliding rate is *independent of wavelength*—in this case the step spacing—when transport is by boundary diffusion.

Gifkins and Snowdon⁶ give an approximate calculation for the sliding rate at a boundary of this shape, assuming boundary-diffusion only. Their result differs from ours by a factor λ/h which can be large, and is incorrect (Ashby *et al.*⁷).

We can also evaluate the sliding rate when volume diffusion is dominant (Gifkins and Snowdon did not consider this). This result* when $D_V \gg D_B (\pi\delta/\lambda)$ is given

*Since steps do not have infinitely sharp corners, the Fourier series describing the stepped shape may be terminated after a finite number of terms. We have made a practice of evaluating the sums of Eqs. [9] and [10] for the first 50 terms of the series.

by

$$\dot{U} = 0.7 \frac{\tau_a \Omega}{kT} \frac{\lambda}{h^2} D_V \quad [15]$$

The sinusoidal boundary, Eq. [11], is a useful standard for comparison: in this case the stepped boundary slides at a rate which is slower by a factor of 0.3 than does the sinusoidal boundary of the same height and wavelength.

d) The General Stepped-Boundary, Allowing Both Boundary and Volume Diffusion

We can now consider the general case of sliding at a boundary containing rectangular steps in it, as a function of the height, h , width w , and spacing λ of the steps, Fig. 3.3(b). This wave-shape is described by the Fourier series

$$x = \sum_1^{\infty} h_n \cos \frac{2\pi}{\lambda} ny \quad [16]$$

with

$$\frac{h_n}{h} = -\frac{2}{n\pi} \sin \frac{n\pi w}{\lambda}$$

and the expression for the sliding rate becomes:

$$\dot{U} = \frac{2}{\pi} \frac{\tau_a \Omega}{kT} \frac{\lambda}{h^2} \frac{D_V}{\sum_1^{\infty} \left\{ \frac{\left(\frac{2}{n\pi} \sin \frac{n\pi w}{\lambda} \right)^2}{\frac{1}{n} + M} \right\}} \quad [17]$$

where, as before,

$$M = \pi \frac{\delta}{\lambda} \frac{D_B}{D_V}$$

Consider first the case of transport by boundary-diffusion only, for which $M \gg 1$. The sliding rate then becomes

$$\dot{U} = 2 \frac{\tau_a \Omega}{kT} \frac{\delta}{h^2} D_B F_1 \left(\frac{w}{\lambda} \right) \quad [18]$$

where

$$F_1 \left(\frac{w}{\lambda} \right) = \frac{1}{\sum_1^{\infty} \left(\frac{2}{n\pi} \sin n\pi \frac{w}{\lambda} \right)^2}$$

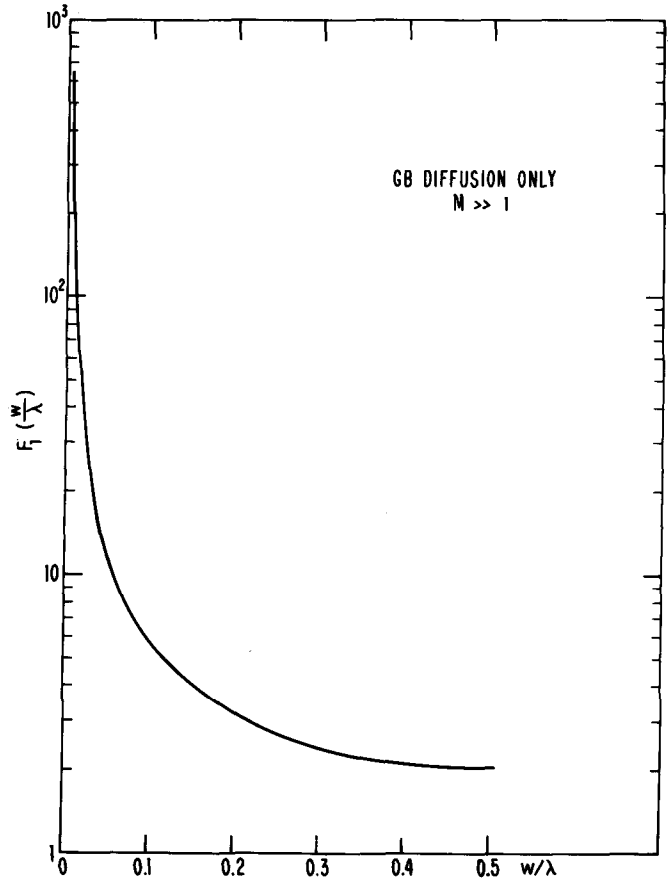


Fig. 3.4—The summation $F_1(w/\lambda)$ for boundary diffusion.

For a given value of w/λ , the function F_1 is a constant, and the sliding rate depends only on the height h of the steps. We have evaluated F_1 as a function of w/λ , and plotted the result as Fig. 3.4 [It shows that narrow “bumps” inhibit sliding far less than the wider ones]. For a given value of w/λ , the corresponding value of F_1 can be read from this plot and plugged into Eq. [18]. For the regular-stepped boundary, for instance, $w/\lambda = 0.5$, and $F_1(w/\lambda) = 2$, leading to the result of Section c) Eq. [14].

In general, no regime exists for which transport is by volume diffusion only. Mathematically, M can play an important role in the summation of Eq. [17] even when it (M) is small. Physically, the reason for this is that even when transport over the basic wavelength λ is by volume diffusion, transport round small steps may still occur mainly by boundary diffusion, and it is this second process that is rate-controlling. Our Eq. [17] correctly takes account of this effect, but it makes the simple presentation of the results predicted by the equation difficult. For this case:

$$\dot{U} = \frac{2}{\pi} \frac{\tau_a \Omega}{kT} \frac{\lambda}{h^2} D_V F_2 \left(\frac{w}{\lambda}, M \right) \quad [19]$$

$$F_2 \left(\frac{w}{\lambda}, M \right) = \frac{1}{\sum_1^{\infty} \left\{ \frac{\left(\frac{2}{n\pi} \sin n\pi \frac{w}{\lambda} \right)^2}{\frac{1}{n} + M} \right\}}$$

Values of $F_2(w/\lambda, M)$ have been computed for a sum of 50 terms and the results, plotted on a logarithmic scale, are given in Fig. 3.5. When the geometry of the

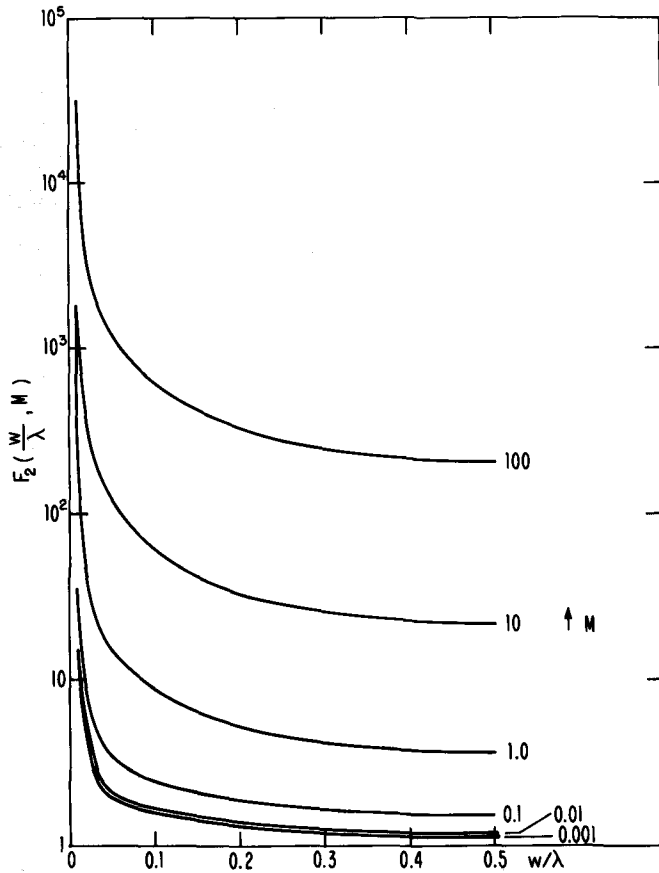


Fig. 3.5—The summation $F_2(w/\lambda, M)$.

boundary is known, and the value of M is known (or can be guessed) then the sliding rate is calculated simply by picking off, from Fig. 3.5, the corresponding value for the summation, which is then plugged into Eq. [19].

e) Creep of a Polycrystal by Grain Boundary Sliding, with Diffusional Accommodation: Comparison with Results Due to Herring⁸ and Coble,⁹ Lifshitz,¹⁰ Gibbs,¹¹ and Green¹²

Consider the deformation of the idealized polycrystalline aggregate shown in Fig. 3.6. When stressed as shown in the figure, this idealized array deforms by two modes of sliding. These are shown by the heavy lines on the figure, and are labeled as Mode 1 and Mode 2. They are orthogonal, so that the net (engineering-shear) strain-rate, $\dot{\gamma}$, is the sum of the strain-rates contributed by each mode. In this way all possible flux paths through the grains of the polycrystal (broken lines on Fig. 3.6) are correctly included.

As pointed out earlier, a good estimate of the sliding rate at a boundary with an obvious basic periodicity is given by approximating its shape by a sine wave of the same periodicity and amplitude. Imagine, then, that both modes are replaced by sine waves of total height $h \approx d/2$ and wavelength $\lambda \approx 2d$. The sliding rate, \dot{U} , for one mode is then given by Eq. [11] and the engineering-shear strain rate, which is the sum of the contributions from the two modes, is

$$\dot{\gamma} = \frac{2\dot{U}}{d} = c \frac{\tau_a \Omega}{kT} \frac{1}{d^2} D_v \left\{ 1 + \frac{\pi \delta}{\lambda} \frac{D_B}{D_v} \right\} \quad [20]$$

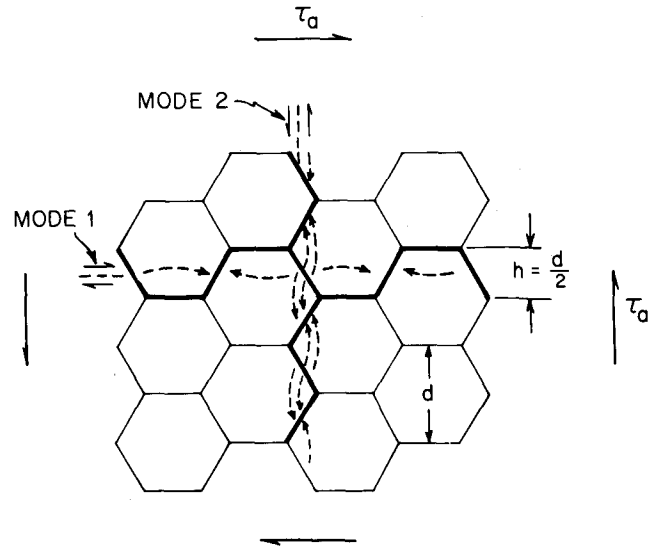


Fig. 3.6—A polycrystal, idealized as an array of hexagons can deform by sliding in two orthogonal modes. Broken lines show the vacancy flux.

where $c = 40$. If, instead, the shapes of the two modes shown on Fig. 3.6 are described by Fourier series, the rate of sliding for each is calculated properly via Eq. [9], and the net strain-rate calculated from the sum, the only change involves the constant c : it is then equal to 42.

To compare our result with those of other authors, it is convenient to reexpress it as follows. A polycrystal which deforms by grain-boundary sliding with diffusional accommodations behaves as if it had a *Newtonian viscosity*, η , defined by

$$\dot{\gamma} = \frac{\tau_a}{\eta} \quad [21]$$

where τ_a is the applied shear stress, and where, for volume diffusion

$$\eta_v = \frac{1}{42} \frac{d^2 kT}{D_v \Omega} \quad [22]$$

and for boundary diffusion

$$\eta_B = \frac{1}{132} \frac{d^3 kT}{\delta D_B \Omega} \quad [23]$$

The deformation of a polycrystal described by these equations is true "diffusional" or "Nabarro-Herring" creep. It is quite clear from the derivation presented here that grain boundary sliding is an integral part of diffusional creep, and that (as Lifshitz¹⁰ has pointed out) without grain boundary sliding no incompatibilities develop, and no diffusional creep is possible.

Herring,⁸ Coble,⁹ and Green¹² have calculated the diffusional strain-rate, and thus the viscosity, of a single spherical grain, when the shear-stress in the plane of its surfaces is relaxed—that is, when grain boundary sliding is permitted. Herring considered transport by volume diffusion, and obtained in our notation

$$\eta_v = \frac{1}{40} \frac{d^2 kT}{D_v \Omega} \quad (\text{Herring})$$

Coble considered* transport by boundary diffusion,

*Gifkins¹⁸ has also presented a calculation of diffusion-controlled deformation, which, physically, is equivalent to that of Coble.

obtaining

$$\eta_B = \frac{1}{141} \frac{d^3 kT}{\delta D_B \Omega} \quad (\text{Coble})$$

(after correcting for a factor of π which was omitted from his paper). These two results are essentially identical with our Eqs. [22] and [23].

A simplified version of the rather complicated calculation of Lifshitz, for the compatible deformation of a polycrystal by volume diffusion, has been presented by Gibbs.¹¹ He obtains

$$\eta_v = \frac{1}{36} \frac{d^2 kT}{D_v \Omega} \quad (\text{Gibbs})$$

which is again essentially identical to Herring's result and to our Eq. [22].

Gibbs, Lifshitz, and our calculation start with a space-filling array of grains, and allow them to deform in a compatible way, so that they fit together both before and after deformation. A physically real consequence of this is that the stress field within the polycrystal is *not uniform*, but varies greatly from point to point in a way which can be calculated, see Appendix 2.

The calculations of Herring, Coble, and Green are less realistic: they avoid the rather complicated compatibility problem by treating a grain with a spherical shape: a shape which does not stack to fill space. Herring correctly points out that the *strain-rate* calculated in this way must be very close to that for equiaxed, space-filling grains, because diffusion smooths out the internal stress field: that is why all the calculations quoted above gave very similar answers. But if one wishes to calculate the *internal stress field* properly, a calculation that incorporates continuity of matter at all stages of the deformation (which those of Herring, Coble, and Green do not) is essential. Our treatment has the further advantage that the effect of grain shape can be calculated, Section 3.2f.

We wish to conclude this section by reemphasizing that "Nabarro-Herring" and "Coble" creep, (which together we call diffusional creep) is *identical* with grain-boundary sliding with diffusional accommodation.*

*A discussion of the role of grain boundary sliding in deformation of polycrystalline materials is given by Gibbs.¹¹

It has been suggested occasionally that grain-boundary sliding and diffusional creep are independent deformation processes, which add. If diffusion is the only mechanism of accommodating the incompatibilities caused by grain-boundary sliding, *diffusional flow and sliding are not independent. They are coupled, and the resulting deformation is correctly described either as "diffusional creep" or as "grain boundary sliding with diffusional accommodation"*. The resulting strain-rate is given by Eq. [20].

If deformation occurs by equal amounts of sliding on two orthogonal systems, as described above, then in a tensile or compression test, grains do not rotate but they *do* change shape, becoming elongated along the tensile direction. If sliding occurs mainly or completely by one mode, then in a tensile or compression

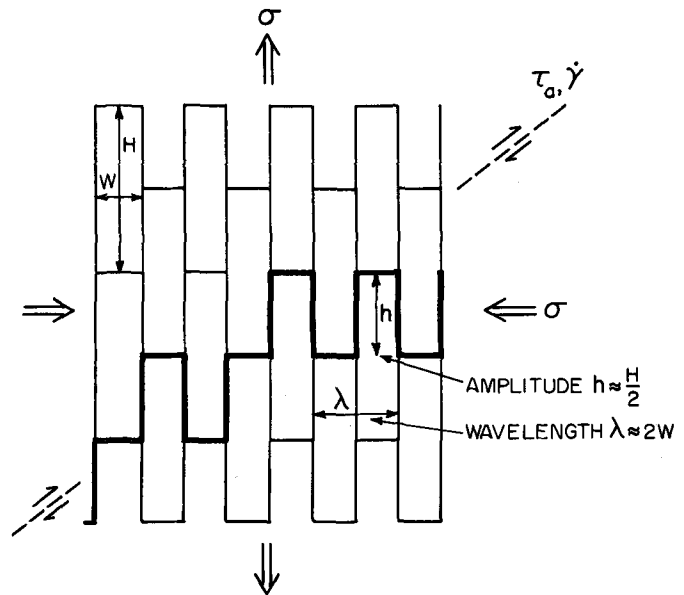


Fig. 3.7—A polycrystal with elongated grains.

test the grains rotate, and *need not* show any elongating or change of shape.

f) The Effect of Grain Shape on Diffusional Creep

Grain shape can have a profound effect on the rate of diffusional creep—that is, of sliding with diffusional accommodation—of a polycrystal. Consider the system of elongated grains shown in Fig. 3.7, in which the grains have height H and width W . Define the aspect ratio R of a grain as $R = H/W$, and the grain size d as $d = (HW)^{1/2}$. Suppose the system is subject to equal, principal tensile and compressive stresses σ : these are equivalent to a shear $\tau_a = \sigma$ at 45 deg to the principal stresses. To a sufficient approximation, the sliding can be considered to occur on a path of wavelength $2W$ and of height $H/2$.

Two regimes emerge, depending on the magnitude of the aspect ratio. Applying the argument which led to Eq. [20] to the elongated grains yields

$$\dot{\gamma} = c \frac{\tau_a \Omega}{kT} \frac{1}{d^2} \left\{ \frac{D_v}{R^2} + \frac{\pi \delta}{d} \frac{D_B}{R^{3/2}} \right\} \quad [24]$$

where c is a constant of about 42. This expression is valid only for grains of low aspect ratio for which $H \approx W$, since otherwise the approximations inherent in Eq. [9] are no longer valid. We note, therefore, that for *small* deviations from an equiaxed shape, the strain-rate attributable to volume and boundary diffusion respectively vary strongly with grain shape:

$$\dot{\gamma}_v \propto \frac{1}{R^2} \quad \text{for } R \approx 1 \quad [25]$$

$$\dot{\gamma}_B \propto \frac{1}{R^{3/2}}$$

From a practical viewpoint, the diffusional creep of a system of very elongated grains ($H \gg W$) is much more interesting. Such structures are obtained in doped tungsten wires and T-D nickel sheet. An approximate calculation of the type given by Cottrell¹³

yields a result appropriate to very elongated grains (Ashby and Raj¹⁴):

$$\dot{\gamma} \approx 16 \frac{\tau_a \Omega}{kT} \frac{1}{d^2} \left\{ \frac{D_v}{R} + \frac{\delta}{d} \frac{D_B}{R^{1/2}} \right\} \quad [26]$$

that is;

$$\dot{\gamma}_v \propto \frac{1}{R} \quad \text{for } R \gg 1 \quad [27]$$

$$\dot{\gamma}_B \propto \frac{1}{R^{1/2}}$$

Note that diffusional creep is minimized by a large grain size with a large aspect-ratio H/W . Since the aspect ratio can be as large as 100, it can significantly change the creep rate.

g) The Effect of Grain Boundary Migration on the Rate of Sliding and Diffusional Creep

Grain boundary sliding in a *bicrystal* is very sensitive to boundary migration. Migration changes the boundary shape, so that the amplitude h and wavelength λ describing the shape change with time. Then, as reference to Eq. [11] shows, the sliding rate will fluctuate with time. We believe that this sort of migration is the cause of the irregular and irreproducible rates of slid-

ing often found in bicrystals of pure metals, and described by Stephens¹⁵ in his review.

The rate of sliding with diffusional accommodation (diffusional creep) of a *polycrystal* is less sensitive to boundary migration. Migration may lead to grain growth at constant shape: then the creep rate decreases with time because d , Eq. [20], is increasing. Or it may lead to change of grain shape, such that boundaries align themselves parallel to the planes of maximum shear stress; though uncommon, such alignment appears during high temperature fatigue, and leads to a rapid increase of strain rate. Finally, local migration may occur with no net change of grain size or shape. The *average* shape of the path along which sliding occurs, like those sketched Fig. 3.6, does not change with time, and the sliding rate with diffusional accommodation is unaffected by the migration.

4.1) SLIDING WITH DIFFUSIONAL ACCOMMODATION

The Three-Dimensional Problem

Up to this point we have considered boundary shapes which were periodic in only one direction—the direction of sliding. But a boundary containing a periodic array of precipitate particles or inclusions, which act like

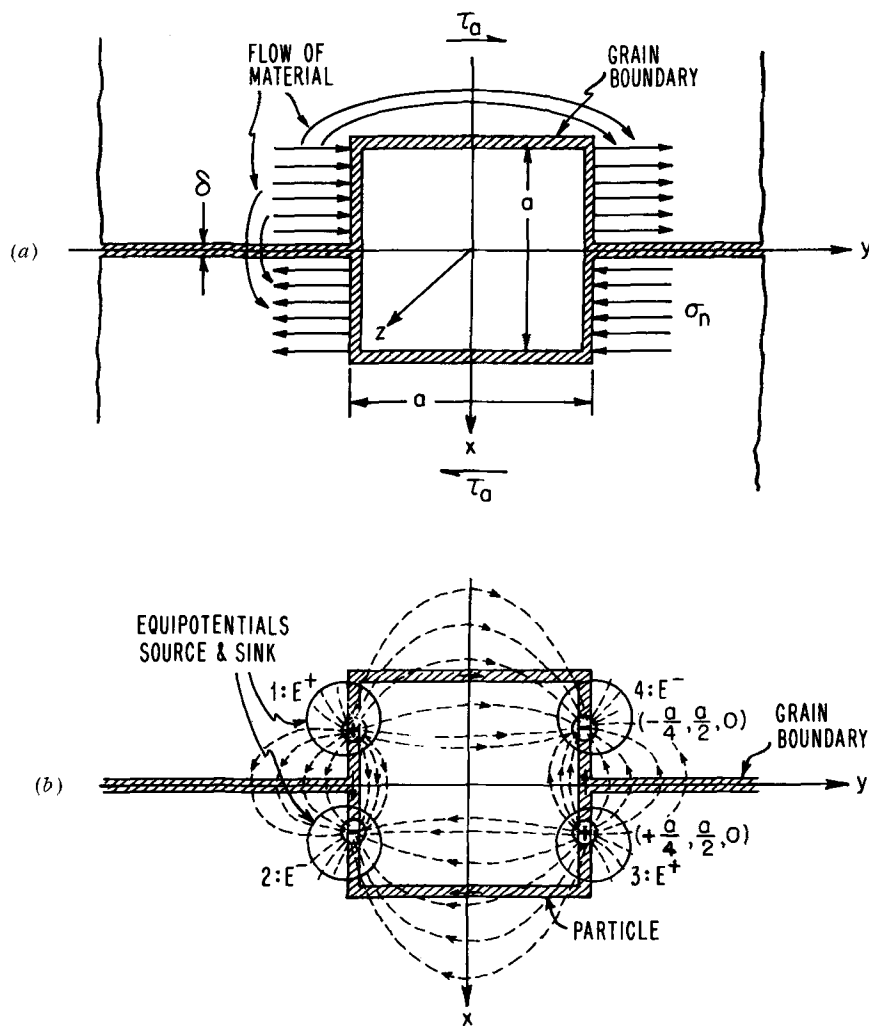


Fig. 4.1—(a) A cube-shaped particle in a grain boundary. (b) The electrostatic analog of (a).

pegs which penetrate the boundary plane, has periodicity in *two* directions. We now consider the problem of the rate of diffusion-controlled sliding at a boundary such as this, one part of which is shown in Fig. 4.1(a). This figure shows a section through single cube-shaped particle, of size a . When an applied shear stress τ_a causes sliding, normal stresses σ_n appear at the faces of each particle. The array of particles then behaves like a periodic array of discrete sinks and sources for vacancies. The diffusion problem can be solved at a sufficient level of approximation by an electrostatic analog: the diffusive flow round a particle, driven by the normal stresses σ_n is analogous to the current flow driven by a suitable distribution of charge, Fig. 4.1(b). This analogy is developed in Appendix 3, where it is shown that the rate of sliding, \dot{U} , at a plane boundary containing an array of discrete impermeable particles of size a and spacing λ is given by

$$\dot{U} = 1.6 \frac{\tau_a \Omega}{kT} \frac{\lambda^2}{a^3} D_v \left\{ 1 + 5 \frac{\delta}{a} \frac{D_B}{D_v} \right\} \quad [28]$$

Here τ_a is the applied shear stress Ω the atomic number, D_v the coefficient of volume self-diffusion, D_B that for diffusion in the interface between the particle and the matrix, δ the thickness of this interface, and kT is Boltzmann's constant times the absolute temperature.

Slight modifications of the expression are required if the particle itself transmits a diffusive flux, and when the particle is coherent in one grain. These are discussed in the Appendix. The equations should not be treated too literally. The approximations involved in their derivation could involve errors of up to a factor of 2. Since diffusion coefficients are not known to this level of accuracy, we feel that the equations are adequate for any practical situation.

4.2) EXAMPLES AND DISCUSSION BASED ON THE RESULTS OF SECTION 4.1

a) The Boundary Containing Discrete Particles: Comparison With the Result of Gibbs¹¹

If the particles are sufficiently small, the quantity

$$\frac{\delta}{a} \frac{D_B}{D_v} \gg 1$$

and the sliding rate is limited by boundary diffusion. (As a rough rule-of-thumb, we anticipate that a particle size of less than 1000Å will lead to boundary diffusion control; a size of more than 10μ to volume-diffusion control; and a size inbetween to control by either volume or boundary diffusion). The sliding-rate is then

$$\dot{U}_B = \frac{8 \tau_a \Omega}{kT} \frac{\lambda^2}{a^4} \delta D_B \quad [29]$$

Note that *big particles (large a) slow down the sliding rate more effectively than the same volume fraction of small particles.*

One earlier calculation of the effect of precipitates on grain boundary sliding exists. Gibbs¹¹ considered sliding limited by boundary-diffusion only, and, by a somewhat less rigorous argument than ours, obtained (in our notation)

$$\dot{U}_B \approx \frac{2 \tau_a \Omega}{kT} \frac{\lambda^2}{a^4} \delta D_B \quad (\text{Gibbs})$$

In all important respects this is identical with our Eq. [29]. The constant differs by a factor of 4.

b) Does Grain Boundary Precipitation Limit the Rate of Diffusional Creep in a Polycrystal?

Continuum calculations, with which this report is mainly concerned, *predict that particles do very little to slow up the macroscopic diffusional creep* of a polycrystal. This conclusion, given earlier by Gibbs,¹¹ can be reached by comparing the sliding rate of a plane boundary containing an array of particles, Eq. [28], with that for a path through a polycrystal, Section 3.2e. For all realistic values of particle size and spacing, it turns out that the grain size, not the particle size, limits the sliding rate.

This conclusion ignores the *microscopic* aspects of diffusional creep. There is some evidence that a dispersion of particles can restrict the ability of a grain boundary to emit or absorb vacancies, and can interfere in other ways with the details, at an atomic level, of the sliding process (Ashby³). Crudely, the result is to introduce a *threshold stress* below which no diffusional creep can occur.

More important, an array of particles (or even of bubbles or voids) can profoundly alter the grain shape, and with it, the sliding rate as described in Section 3.2f. The classic example appears to be that of tungsten wire. Pure tungsten (and most other bcc metals) readily forms a bamboo structure, consisting of nearly planar boundaries. A dispersion of bubbles introduced by "doping" (which alone cannot hinder the sliding process) or of thoria, results in elongated, interlocked, and extremely wavy grains, with a great resistance to sliding deformation.

5) SUMMARY

1) Grain boundaries are seldom perfectly planar. When a shear stress causes sliding to occur at a grain boundary, some accommodation process is necessary where the boundary deviates from a perfect plane. This process almost always determines the extent and rate of sliding.

2) The accommodation may be purely elastic; or it may be diffusional; or it may involve plastic flow by dislocation motion. This paper considers in detail the elastic and diffusional accommodation required when a boundary of arbitrary shape slides.

3) When accommodation is *purely elastic*, internal stresses grow as sliding proceeds, until the appropriate component of them exactly balances the applied stress, when sliding stops. The paper contains equations which give the total amount of sliding at a boundary of arbitrary shape, and the internal stress-field developed by the sliding, Section 2.1.

4) These equations are applied, in Section 2.2 to a) a boundary of sinusoidal shape, b) a saw-tooth and a stepped boundary, and c) a polycrystal; it is shown that the total amount of sliding is usually very small, but it leads to an apparently lower shear modulus (Zener relaxation). Its rate is related to the intrinsic viscosity of the boundary plane, but since its magnitude is small, most measurements of sliding rate do not measure this intrinsic viscosity (internal friction is an exception).

5) When accommodation is by *diffusive flow of matter* from one part of the boundary to another, a different internal stress field is set up. The paper contains equations for the rate of sliding, and the stress field, at a boundary of arbitrary shape when accommodation is diffusional. Both bulk and boundary diffusion are considered, Sections 3.1 and 4.1.

6) These equations are applied to:

a) A boundary of sinusoidal shape.

b) A stepped boundary, with periodic, symmetrical steps; the results are compared with a more limited calculation due to Gifkins and Snowdon, which we consider to be incorrect.

c) A more general, unsymmetrical stepped boundary.

d) The creep of a polycrystal by grain boundary sliding with diffusional accommodation; this is true diffusional creep. The results are compared with, and agree well with, those of Herring, Coble, Lifshitz, Gibbs, and Green.

e) The effect of grain shape on diffusional creep: elongated grains can greatly retard it.

f) The effect of grain boundary migration on diffusional creep: in a polycrystal the effect is generally small unless grain growth occurs; in a bicrystal the effect can be large, and lead to an irregular sliding rate.

g) The rate of sliding at a planar grain boundary containing precipitate particles or inclusions; the result is compared with, and supports the form of, a more limited result due to Gibbs.

h) The influence of precipitates or inclusions on the diffusional creep of a polycrystal; the effect is usually small, though microscopic processes and the effect of particles on grain shape may influence it, Sections 3.2 and 4.2.

ACKNOWLEDGMENTS

This work was supported in part by the Advanced Research Projects Agency under Contract SD-88, in part by the Office of Naval Research under Contract N00014-67-A-0298-0020, and by the Division of Engineering and Applied Physics, Harvard University. We particularly wish to acknowledge the help of Mr. H. J. Frost whose suggestions contributed to the solution of the diffusion problem of Section 3, and to Professor F. A. McClintock and Professor J. W. Hutchinson for stimulating and helpful discussions.

APPENDIX 1

SLIDING WITH ELASTIC ACCOMMODATION

The Two-Dimensional Problem

If the shape of any grain boundary has a two-fold axis of symmetry and has bounded first derivatives, it may be described by a cosine Fourier series:

$$x = \sum_1^{\infty} h_n \cos \frac{2\pi}{\lambda} ny \quad [A1]$$

The thickness of the bicrystal in a direction normal to the boundary plane is considered to be large compared to λ , (the basic wavelength of the boundary shape) so that conditions of plane strain apply. A shear stress τ_a is applied in the y direction as shown in Fig. 2.1,

causing the upper half-crystal to slide over the lower one in the boundary plane. The net relative displacement of the two crystals, parallel to the y -axis, is \bar{U} which we imagine as a displacement of $\frac{1}{2}\bar{U}$ of the upper half-crystal to the right, and an equal displacement of the lower one to the left. For convenience we consider only the lower crystal, *i.e.* the region $-\infty \leq y \leq \infty$, $+\infty \leq x \leq 0$. As a result of the symmetry of the problem the displacements, stresses, and sliding in the upper crystal are complementary. If each half-crystal were rigid, then a sliding displacement $\bar{U}/2$ of one half-crystal would produce tangential displacements \bar{U}_t and normal displacements \bar{U}_n in the boundary surface, where

$$\left. \begin{aligned} \bar{U}_t &= \frac{\bar{U}}{2} \cos \theta \approx \frac{\bar{U}}{2} \\ \bar{U}_n &= \frac{\bar{U}}{2} \sin \theta \approx \frac{\bar{U}}{2} \frac{dx}{dy} \\ &= -\bar{U} \frac{\pi}{\lambda} \sum_1^{\infty} n h_n \sin \frac{2\pi}{\lambda} ny \end{aligned} \right\} \quad [A2]$$

The assumption here that θ is sufficiently small that $\cos \theta \approx 1$ and $\sin \theta \approx \tan \theta$, can introduce errors of order $\sqrt{2}$ only when the amplitude h of the boundary exceeds half the wavelength λ . We normally consider boundaries for which $h \ll \lambda$.

Suppose now that some distribution of normal stress, σ_n , acts across the boundary as shown in Fig. 2.1. Let this be described by a Fourier series, which by symmetry must have the form

$$\sigma_n = \gamma \sum_1^{\infty} \alpha_n \sin \frac{2\pi}{\lambda} ny \quad [A3]$$

where γ has the dimensions of stress, and the α 's are numerical coefficients to be determined. Mechanical equilibrium in the boundary plane requires that

$$\tau_a \lambda - \int_{-(\lambda/2)}^{+(\lambda/2)} \sigma_n \frac{dx}{dy} dy = 0 \quad [A4]$$

which leads to the following value for γ :

$$\gamma = - \frac{\tau_a \lambda}{\pi \sum_1^{\infty} n \alpha_n h_n} \quad [A5]$$

The procedure for evaluating α_n is straightforward, but messy. It involves calculating the displacement field due to the normal stress distribution of Eq. [A3], and equating the appropriate component to that caused by sliding, as follows. We have assumed the boundary to have a small amplitude-to-wavelength ratio. If we now assume the boundary to be flat but apply to it the same boundary conditions as we did to the wave-like boundary, we introduce only second-order errors. The vectors \mathbf{n} and \mathbf{t} now coincide with our "x" and "y" axes. We may now use a standard result of elasticity theory (Timoshenko and Goodier¹⁶), namely that, under conditions of plane strain, a sinusoidal surface stress $\sigma_x(0, y) = \alpha \sin(2\pi/\lambda)y$, $\tau_{xy}(0, y) = 0$ leads to the following internal stress distribution:

$$\sigma_x = \alpha \left[1 + \frac{2\pi}{\lambda} x \right] e^{-(2\pi/\lambda)x} \sin \frac{2\pi}{\lambda} y$$

The Two-Dimensional Problem

$$\begin{aligned} \sigma_y &= \alpha \left[1 - \frac{2\pi}{\lambda} x \right] e^{-(2\pi/\lambda)x} \sin \frac{2\pi}{\lambda} y \\ \tau_{xy} &= -\alpha \frac{2\pi}{\lambda} x e^{-(2\pi/\lambda)x} \cos \frac{2\pi}{\lambda} y \\ \sigma_z &= \nu(\sigma_x + \sigma_y) \end{aligned} \quad [A6]$$

Applied to the general boundary shape, these become:

$$\begin{aligned} \sigma_x &= \gamma \sum_1^\infty \alpha_n \left[1 + \frac{2\pi}{\lambda} nx \right] e^{-(2\pi/\lambda)nx} \sin \frac{2\pi}{\lambda} ny \\ \sigma_y &= \gamma \sum_1^\infty \alpha_n \left[1 - \frac{2\pi}{\lambda} nx \right] e^{-(2\pi/\lambda)nx} \sin \frac{2\pi}{\lambda} ny \\ \tau_{xy} &= -\gamma \sum_1^\infty \alpha_n \frac{2\pi}{\lambda} nxe^{-(2\pi/\lambda)nx} \cos \frac{2\pi}{\lambda} ny \\ \sigma_z &= \nu[\sigma_x + \sigma_y] \end{aligned} \quad [A7]$$

where $-\infty \leq y \leq \infty$
 $+\infty \leq x \leq 0$

Applying the constitutive relations to Eqs. [A7] we obtain the elastic strains:

$$\begin{aligned} \epsilon_x &= \frac{(1+\nu)}{E} \gamma \sum_1^\infty \alpha_n \left[(1-2\nu) + \frac{2\pi}{\lambda} nx \right] e^{-(2\pi/\lambda)nx} \\ &\quad \times \sin \frac{2\pi}{\lambda} ny \\ \epsilon_y &= \frac{(1+\nu)}{E} \gamma \sum_1^\infty \alpha_n \left[(1-2\nu) - \frac{2\pi}{\lambda} nx \right] e^{-(2\pi/\lambda)nx} \\ &\quad \times \sin \frac{2\pi}{\lambda} ny \\ \epsilon_{xy} &= \frac{-(1+\nu)}{E} \gamma \sum_1^\infty \alpha_n \frac{2\pi}{\lambda} nxe^{-(2\pi/\lambda)nx} \\ &\quad \times \cos \frac{2\pi}{\lambda} ny \end{aligned}$$

where E is Young's modulus and ν is Poisson's ratio. The normal displacement of the boundary surface is calculated from

$$\epsilon_{xy} = \frac{1}{2} \left[\frac{\partial u_x}{\partial y} + \frac{\partial u_y}{\partial x} \right]$$

Differentiating with respect to y and rearranging terms we obtain

$$\frac{\partial^2 u_x}{\partial y^2} = 2 \frac{\partial \epsilon_{xy}}{\partial y} - \frac{\partial \epsilon_y}{\partial x} \quad \text{where } x > 0$$

This yields:

$$\left(\frac{\partial^2 u_x}{\partial y^2} \right)_{0,y} = \frac{(1-\nu^2)}{E} \gamma \sum_1^\infty \alpha_n \frac{4\pi n}{\lambda} \sin \frac{2\pi ny}{\lambda}$$

Integration gives:

$$u_x(0, y) = \frac{-2(1-\nu^2)}{E} \gamma \frac{\lambda}{2\pi} \sum_1^\infty \frac{\alpha_n}{n} \sin \frac{2\pi ny}{\lambda} \quad [A8]$$

Equating this elastic displacement to the normal displacement of equation [A2], and equating coefficients (since the equation must hold for all y), we obtain:

$$\alpha_n = n^2 h_n$$

Substituting this into the equation for u_x , and the Eq. [A3] for σ_n , leads immediately to the results [2] and [3] of Section 2. The stress fields within the crystals can be obtained via Eq. [A7].

Consider steady-state sliding at a general boundary with a shape described by the Fourier series, Eq. [1]. During steady-state sliding, vacancies are neither created nor absorbed within the two crystals: the boundary is the only source or sink. This means that the divergence of the flux, $\text{div } \bar{J}$, is zero within both crystals, or, equivalently, that the Laplacian of the chemical potential, μ , be zero within each crystal:

$$\nabla^2 \mu(x, y) = 0 \quad [B1]$$

The flux field for vacancies within the crystals is obtained by solving this equation subject to boundary conditions which ensure chemical equilibrium, mechanical equilibrium, and continuity (or compatible deformation) in the boundary.

Chemical equilibrium in the boundary plane means that the chemical potential μ of vacancies at, and immediately adjacent to a point on the boundary is related to the normal stress σ_n acting on the boundary at that point:

$$\mu = \mu_0 - \sigma_n \Omega \quad (\text{at the boundary}) \quad [B2]$$

where Ω is the atomic volume, and μ_0 the chemical potential appropriate to a stress-free reference state.

As in Appendix 1, let the distribution of normal stress, σ_n , acting across the boundary surface, be described by the Fourier series [A3]. Then *mechanical equilibrium* leads, as before, to the relationship [A5]. Here, however, the parallelism with Appendix 1 ends: the coefficients α_n are determined here by solution of the diffusion equation, and are quite different from those obtained via Hookes law in Appendix 1.

Solution of Eq. [B1] subject to these boundary conditions still leaves the coefficients α_n as unknowns. These are determined by the *continuity condition*, which we now derive. Steady-state sliding requires that the flux of atoms (or counter-flux of vacancies) into each element of the boundary precisely account for the change in volume of the element due to sliding. The element E of Fig. 3.1 is shown in detail in Fig. B1. It has width ΔS . In time element Δt the sliding displacement is $\bar{u}\Delta t$ and a volume $\Delta S \bar{u} \Delta t \sin \theta$ of matter must be pumped out of the element. From here on we approximate the boundary as the plane $(0, y)$ introducing

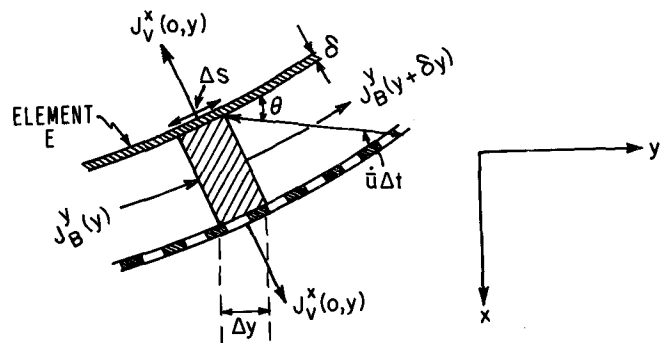


Fig. B1—Details of the element E of Fig. 3.1. Vacancies enter and leave the element via a boundary flux J_B , and a flux through the crystal J_v .

only errors of second order if $h \ll \lambda$, and errors of order $\sqrt{2}$ when $h \approx \lambda/2$. The continuity equation, which can be understood by referring to Fig. B1 is then

$$\begin{aligned} \dot{U} \Delta t \Delta S \sin \theta = \Omega \Delta t \{ & -2J_v^x(0, y) \Delta S \\ & - [J_B^y(y + \Delta y) - J_B^y(y)] \delta \} \end{aligned} \quad [\text{B3}]$$

Here J_v^x is the volume diffusion flux of vacancies: since vacancies are generated or absorbed only at the boundary, this flux at the boundary plane has an x -component only. J_B^y is the diffusional flux of vacancies in the plane of the grain boundary; it has a y -component only. δ is the thickness of the grain boundary and measures the area across which the boundary flux passes. The atomic volume is Ω .

Applying our usual approximation that the slope of the boundary, $\tan \theta = dx/dy \approx \sin \theta$ and that $\Delta S/\Delta y = \cos \theta \approx 1$, and allowing the incremental distances Δy and so forth to become infinitesimal, gives for the continuity equation:

$$-J_v^x(0, y) - \frac{\delta}{2} \frac{dJ_B^y}{dy} = \frac{\dot{U}}{2\Omega} \frac{dx}{dy} \quad [\text{B4}]$$

The diffusional fluxes of vacancies are related to the gradients of chemical potential by

$$\left. \begin{aligned} \bar{J}_v(x, y) &= -\frac{D_v}{\Omega kT} \bar{\nabla} \mu(x, y) \\ J_B^y(y) &= -\frac{D_B}{\Omega kT} \frac{d\mu}{dy}(0, y) \end{aligned} \right\} \quad [\text{B5}]$$

where D_v is the self-diffusion coefficient for volume diffusion, D_B is that for boundary diffusion,* and k is

*Strictly speaking, the correct diffusion coefficients D_v/f_v and D_B/f_B should be employed; here D_v and D_B are the tracer diffusion coefficients and f_v and f_B are the correlation factors. A reader requiring an exact solution should make this replacement. For simplicity in this paper the correlation factors are assumed to be close to unity, and are omitted.

Boltzmann's constant and T the absolute temperature.

We may now reformulate the problem as follows. We require a solution to the equation

$$\nabla^2 \mu(x, y) = 0$$

Subject to the boundary conditions

$$\left. \begin{aligned} \mu(0, y) &= \mu_0 - \Omega \gamma \sum_1^{\infty} \alpha_n \sin \frac{2\pi}{\lambda} ny \\ \mu(\infty, y) &= \mu_0 \end{aligned} \right\} \quad [\text{B6}]$$

The appropriate solution has the form

$$\mu(x, y) = \sum_1^{\infty} A_n \exp - \left(\frac{2\pi nx}{\lambda} \right) \sin \frac{2\pi ny}{\lambda} + C$$

Applying the boundary conditions, which hold for all y , leads to

$$C = \mu_0$$

$$A_n = -\Omega \gamma \alpha_n$$

Substituting in Eqs. [B5] gives the fluxes

$$\begin{aligned} J_v^x(0, y) &= + \frac{D_v}{\Omega kT} \Omega \gamma \sum_1^{\infty} - \frac{2\pi n}{\lambda} \alpha_n \sin \frac{2\pi ny}{\lambda} \\ \frac{dJ_B^y}{dy}(0, y) &= + \frac{D_B}{\Omega kT} \Omega \gamma \sum_1^{\infty} - \left(\frac{2\pi n}{\lambda} \right)^2 \alpha_n \sin \frac{2\pi ny}{\lambda} \end{aligned}$$

Substituting these into the continuity equation [B4] yields

$$\begin{aligned} \frac{\gamma}{kT} \sum_1^{\infty} \alpha_n \left(nD_v + \frac{\pi\delta}{\lambda} n^2 D_B \right) \sin \frac{2\pi}{\lambda} ny \\ = - \frac{\dot{U}}{2\Omega} \sum_1^{\infty} n h_n \sin \frac{2\pi}{\lambda} ny \end{aligned}$$

This equation must also hold for all values of y , so that

$$\alpha_n = \frac{1}{K} \left\{ \frac{h_n}{D_v + \frac{\pi\delta}{\lambda} n D_B} \right\} \quad [\text{B7}]$$

and

$$\dot{U} = - \frac{2\gamma\Omega}{kT} \frac{1}{K} \quad [\text{B8}]$$

Here K is an arbitrary constant. By substituting for γ in Eq. [B8] and eliminating K and α_n , Eq. [B7] yields a final expression for the sliding rate, \dot{U} , presented in the text Eq. [9]. A similar substitution into Eq. [A3] yields the distribution of normal stress, presented as Eq. [10]. The entire stress field within each crystal, if it is desired, can be obtained by inserting the expressions for γ and α_n into Eqs. [A7].

APPENDIX 3

SLIDING WITH DIFFUSIONAL ACCOMMODATION

The Three-Dimensional Problem

A) THE ELECTROSTATIC ANALOG

Consider a boundary containing well-separated cubic particles; one is shown in Fig. 4.1(a). We first solve the analogous electrostatic problem, Fig. 4.1(b), replacing the stressed body by a body having a finite specific conductivity, and containing sources and sinks for charge. These sources and sinks we imagine as electrodes held at a potential difference ΔV . Then the current I flowing between the electrodes is:

$$I = K \Delta V \quad [\text{C1}]$$

where K is the conductivity of the body as seen by the electrodes. Each electrode forms an equipotential, and the current flow is normal to its surface. We approximate the diffusion field by the analogous electrostatic field due to four point charges of strength $\pm q$, placed at coordinates $[\pm(a/4), \pm(a/2), 0]$ which form the centers of the faces of the upper and lower halves of the particle. From Gauss' Law these charges may be replaced by four nearly spherical equipotential surfaces E^\pm , containing the charges $\pm q$. We will assume that the centers of these surfaces lie on the surface of the particle, and that they pass through the points $[\pm(a/2), \pm(a/2), 0]$ as shown in the figure. (We have tried other geometries, and find that the final result is insensitive to assumptions concerning the form of the equipotentials.)

The conductance K of the body can be calculated from the equivalent electrostatic problem (Reitz and Milford¹⁷) and is:

$$K = \frac{\kappa | Q |}{\epsilon | \Delta V |} \quad [\text{C2}]$$

where κ is the specific conductance, ϵ is the dielectric

constant and $|Q|$ the total charge; thus $|Q| = \Sigma |q|$. $|\Delta V|$ is the potential difference between the electrodes. This we obtain from the potential function $V(x, y, z)$, which is the algebraic sum of the potentials due to each of the four point charges thus:

$$V(x, y, z) = (V_1 + V_2 + V_3 + V_4)$$

where V_1 and so forth are the potentials due to charges number 1, 2, 3, and 4 as shown on Fig. 4.1(b):

$$V_1 = -\frac{q}{\epsilon} \frac{1}{\left[\left(x + \frac{a}{4}\right)^2 + \left(y + \frac{a}{2}\right)^2 + z^2\right]^{1/2}}$$

and so on. The required potential difference between two of the equipotential surfaces is $|\Delta V| = |E^+ - E^-|$ where

$$|E^+| = |E^-| = |V\left(\pm \frac{a}{2}, \pm \frac{a}{2}, 0\right)|$$

$|\Delta V|$ is easily evaluated as

$$\Delta V = \frac{4.8}{a} \frac{q}{\epsilon}$$

Substituting this into Eq. [C2], and noting that $|Q| = 4q$ we have

$$K_v = 0.83a\kappa_v$$

where K_v is the bulk, or volume conductivity of the body containing the electrodes, and κ_v is the specific volume conductivity.

Transport by grain boundary diffusion implies specific boundary conductance κ_B which differs from that of the volume. For this case the standard relation between conductance and specific conductance can be used, giving

$$K_B = 2\delta\kappa_B$$

where δ is the thickness of the high conductivity layer, that is, the boundary thickness. Thus the net conductivity of the body is

$$K = 0.8a\kappa_v + 2\delta\kappa_B \quad [C3]$$

In many diffusion problems the particle is composed of a chemically different material through which no diffusive flux passes, *i.e.* the particle is impermeable. This lowers the volume conductivity by a factor which we will assume to be 0.5, giving for the net conductivity $(0.4a\kappa_v + 2\delta\kappa_B)$.

Finally, many real systems contain particles which are coherent with one grain, but incoherent with the other. Presumably the coherent surfaces cannot act as sinks and sources. The electrostatic analog becomes a pair of point charges, 1 and 4 in Fig. 4.1(b), instead of four. The resulting conductance, for a permeable particle becomes $(0.3a\kappa_v + \delta\kappa_B)$ and for an impermeable one $(0.15a\kappa_v + \delta\kappa_B)$.

B) APPLICATION TO THE DIFFUSION PROBLEM

Comparing the equation for the electric flux

$$\bar{J} = -\kappa \bar{\nabla} V$$

with that for diffusive flux

$$\bar{J} = -\frac{D}{\Omega kT} \bar{\nabla} \mu$$

where $\bar{\nabla} V$ and $\bar{\nabla} \mu$ are respectively the gradients of

electric and chemical potential, we find

$$\kappa_v = \frac{D_v}{\Omega kT}$$

$$\kappa_B = \frac{D_B}{\Omega kT}$$

where D_v and D_B are the volume and boundary diffusivities. Inserting these expressions into Eq. [C3] gives the "diffusive conductance" K_{Dif} of the body. The total flow of vacancies round the particle is related to the difference in potential $\Delta\mu$ between the two sides of the particle by

$$I = K_{\text{Dif}} \Delta\mu \quad [C4]$$

(I is a number of vacancies flowing round the particle per sec).

Suppose the sliding rate at the boundary is \dot{U} . Then conservation of matter requires that

$$I = \frac{\dot{U} a^2}{2\Omega} \quad [C5]$$

We relate the chemical potential difference $\Delta\mu$ to the applied stress τ_a by an energy argument. We require that during an increment of sliding $\dot{U} \delta t$, the external work $\tau_a \dot{U} \delta t$ is equal to the energy dissipated within the body. This is $I \delta t \Delta\mu N$, where N is the number of particles of size a per unit area of boundary. This leads to

$$\tau_a \dot{U} = IN \Delta\mu \quad [C6]$$

Solving these equations for \dot{U} gives

$$\dot{U} = \frac{4\Omega^2 K_{\text{Dif}} \tau_a}{Na^4} \quad [C7]$$

Inserting appropriate values for the diffusional conductance K_{Dif} from Eqs. [C3], and replacing N by $1/\lambda^2$ where λ is the particle spacing, we obtain

$$\dot{U} = 3.2 \frac{\tau_a \Omega}{kT} \frac{\lambda^2}{a^3} D_v \left\{ 1 + 2.5 \frac{\delta D_B}{a D_v} \right\} \quad [C8a]$$

for a permeable particle, incoherent in both grains;

$$\dot{U} = 1.6 \frac{\tau_a \Omega}{kT} \frac{\lambda^2}{a^3} D_v \left\{ 1 + 5 \frac{\delta D_B}{a D_v} \right\} \quad [C8b]$$

for an impermeable particle (*i.e.* one through which no diffusion can occur) incoherent in both grains; and so on.

REFERENCES

1. R. Raj: Ph.D. Thesis, Harvard University, Feb. 1971, to be published.
2. H. Gleiter, E. Hornbogen, and G. Baro: *Acta Met.*, 1964, vol. 16, p. 1053.
3. M. F. Ashby: *Scripta Met.*, 1969, vol. 3, p. 837.
4. C. Zener: *Phys. Rev.*, 1941, vol. 60, p. 906.
5. T. S. Kê: *Phys. Rev.*, 1947, vol. 71, p. 533.
6. R. C. Gifkins and K. U. Snowdon: *Nature*, 1966, vol. 212, p. 916.
7. M. F. Ashby, R. Raj, and R. C. Gifkins: *Scripta Met.*, 1970, vol. 4, p. 737.
8. C. Herring: *J. Appl. Phys.*, 1950, vol. 21, p. 437.
9. R. L. Coble: *J. Appl. Phys.*, 1963, vol. 34, p. 1679.
10. L. M. Lifshitz: *Soviet Phys. JETP*, 1963, vol. 17, p. 909.
11. G. B. Gibbs: *Mem. Sci. Rev. Met.*, 1965, vol. 62, p. 781; *Mater. Sci. Eng.*, 1967-68, vol. 2, p. 269.
12. H. W. Green: *J. Appl. Phys.*, 1970, vol. 41, p. 3899.
13. A. H. Cottrell: *Mechanical Properties of Matter*, p. 202, John Wiley & Sons, New York, 1964.
14. M. F. Ashby and R. Raj: Harvard University Report No. 2, June 1970.
15. R. N. Stephens: *Met. Rev.*, 1966, vol. 11, p. 129.
16. S. P. Timoshenko and J. N. Goodier: *Theory of Elasticity*, Ch. 3, pp. 35-64, McGraw Hill, New York, 1970.
17. J. R. Reitz and F. F. Milford: *Foundations of Electromagnetic Theory*, Ch. 7, Addison Wesley, Reading, Mass., 1964.
18. R. C. Gifkins: *J. Inst. Metals*, 1967, vol. 95, p. 373.